Extended Abstracts of the 2002 International Conference on Solid State Devices and Materials, Nagoya, 2002, pp. 810-811

F-7-3

Fabrication of AlGaN/GaN Quantum Wires by ECR-RIBE Process and Their Electrical Properties

Tsutomu Muranaka, Zhi Jin, Makoto Endo, Tamotsu Hashizume and Hideki Hasegawa

Research Center for Integrated Quantum Electronics and Graduate School of Electronics and Information Engineering, Hokkaido University, North-13, West-8, Sapporo 060-8628, JAPAN
TEL: +81-11-706-7176, FAX: +81-11-716-6004, e-mail: muranaka@rciqe.hokudai.ac.jp

1. Introduction

Owing to its large conduction band offset and high sheet carrier densities, the AlGaN/GaN heterostructure system is suited, not only to conventional photonic and HEMT applications, but also to nanostructure devices operating at high temperatures. Since low-damage wet chemical etching, often used in GaAs- and InP-based nanostructures, is not applicable to GaN-based materials, a low-damage and well-controllable dry etching process becomes a key for nano-fabrication. For this purpose, we have recently developed an electron cyclotron resonance-reactive ion beam etching (ECR-RIBE) process for GaN using a methane-based gas mixture [1,2].

The purpose of this paper is to further extend our ECR-RIBE process to dry etching of AlGaN/GaN wafers, and to attempt to fabricate AlGaN/GaN quantum wires by the optimized dry etching process.

2. Experimental

The sample structures used in this study are shown in **Fig. 1**. The planar $Al_xGa_{1-x}N$/GaN (x=0.25-0.3) heterostructure sample shown in **Fig. 1(a)** grown by MOVPE was used for characterization and optimization of the ECR-RIBE process. The cross-sectional structure of the quantum wire sample produced by dry etching is shown in **Fig. 1(b)**. Etching was performed in an ECR-RIBE chamber described in ref. [1]. This chamber was connected to an ultrahigh vacuum (UHV) multi chamber system where *in-situ* XPS and PL characterization of the samples without breaking vacuum was possible.

The etching masks were thin PCVD-SiO_2 films patterned by electron-beam (EB) lithography. The basic gas mixture for etching was that of methane (CH_4), hydrogen (H_2) and argon (Ar). A particular attention was paid on the effects of nitrogen (N_2) addition, following the previous successful experience on GaN etching [1,2] as well as on InP etching [3]. The microwave power was 200 W and the acceleration voltage was 300 V.

The etching profiles and surface morphology were characterized by AFM and SEM observations. Chemical and optical properties were characterized by *in-situ* XPS and PL. The electrical properties of wires were investigated by I-V and Shubnikov-de Haas (SdH) measurements.

3. Results and Discussion

3.1 Optimization of Etching Process for AlGaN/GaN

Our ECR-RIBE process successfully etched AlGaN/GaN wafers. The observed etching depth is compared vs. time in **Fig. 2** for the cases of without and with N_2 addition. The etching depth saturated at 400 nm without N_2. This saturation disappeared with N_2 gas, giving a constant and relatively small etching rate of 9 nm/min suitable for controlled formation of nanostructures.

A relatively poor AFM surface morphology shown in **Fig. 3(a)** with rms roughness of 4 nm was remarkably improved by addition of N_2 as seen in **Fig. 3(b)**. As shown in **Fig. 4(a)**, XPS spectra from the surface before etching had higher binding energy shoulders due to natural oxides of AlGaN. After etching without N_2, the surface became oxide-free, but it had Ga-Ga bonding peaks and a large change in intensity ratio of Ga-N and Al-N, as seen in **Fig. 4(b)**. With N_2, such anomalies disappeared, as shown in **Fig. 4(c)**. PL results are summarized in **Fig. 5**. As a reference, PL from GaN surface is shown in **Fig. 5(a)** where the band-edge emission near 3.4 eV and a so-called yellow broad luminescence centered at 2.2 eV are seen. After etching AlGaN/GaN without N_2 gas, the band edge emission from GaN drastically decreased as shown in **Fig. 5(b)** possibly due to non-stoichiometric phase including defects causing efficient non-radiative recombination. On the other hand, after etching with N_2, the GaN band-edge emission remained, as shown in **Fig. 5(c)**.

Thus, the methane-based ECR-RIBE process works excellently on the AlGaN/GaN wafer with N_2 addition. The empirical optimum gas make-up was found to be $CH_4/H_2/Ar/N_2$ = 5/15/3/3 sccm.

3.2 Fabrication and Electrical Characterization of AlGaN/GaN Quantum Wires

Using the optimized dry etching process, $<1\bar{1}00>$-oriented AlGaN/GaN quantum wires having different geometrical widths, W_{geo}, were fabricated. An example of AFM image of a wire with W_{geo}= 600 nm is shown in **Fig. 6**. Smooth $\{11\bar{2}1\}$ side facets were formed by etching, showing chemical nature of etching with low process-induced damage rather than physical bombardment-induced etching.

Observed width dependence of wire conductance is shown in **Fig. 7(a)**, showing a linear dependence as expected for 20 –300 K. Under strong magnetic fields, clear SdH oscillations were observed, indicating occurrence of fairly coherent cyclotron motions in the structure. The resultant Landau plot is shown in **Fig. 7(b)**. Marked deviation from linear behavior indicates presence of one-dimensional constriction. A simple analysis gave values of sheet carrier concentration of 4.8 x 10^{12} cm^{-2} and an effective wire width of 130 nm for a wire with W_{geo} = 400 nm. Thus, there seems to exist significant surface depletion widths due a strong Fermi level pinning on the etched side facets of the wire, being similarly to the case of GaAs-based materials.

References

[1] Z. Jin et al.: Appl. Sur. Sci. **190**, 361 (2002)
[2] M. Endo et al.: to appear in Jpn. J. Appl. Phys. (2002)
[3] Z. Jin et al.: Jpn. J. Appl. Phys. **40**, 2757 (2001)

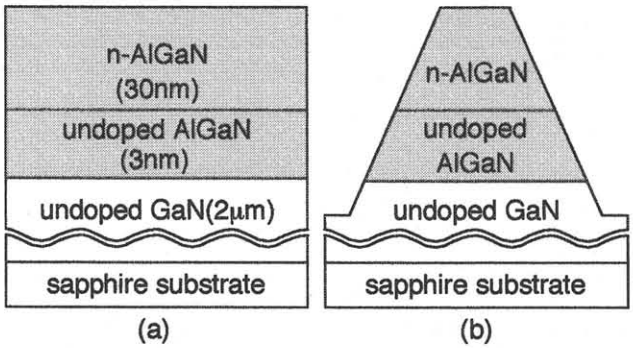

Fig.1 Sample structures used in this study. (a) AlGaN/GaN heterostructure sample and (b) quantum wire sample.

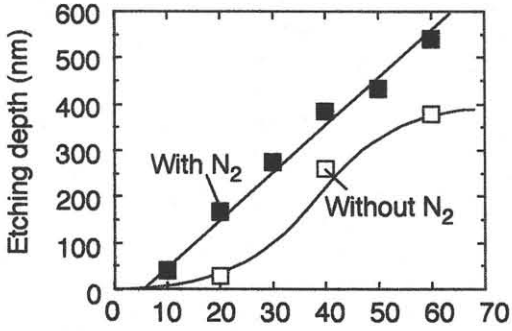

Fig. 2 Relationship of etching depth and etching time for AlGaN/GaN structures.

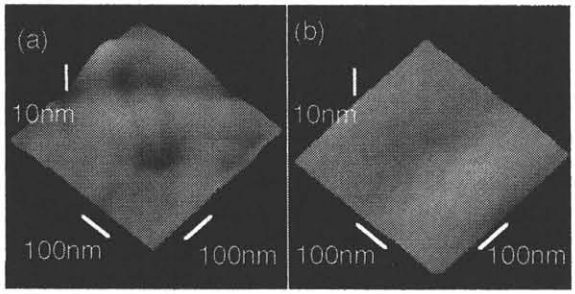

Fig. 3 AFM images of AlGaN/GaN surface after etching (a) without N_2 and (b) with N_2.

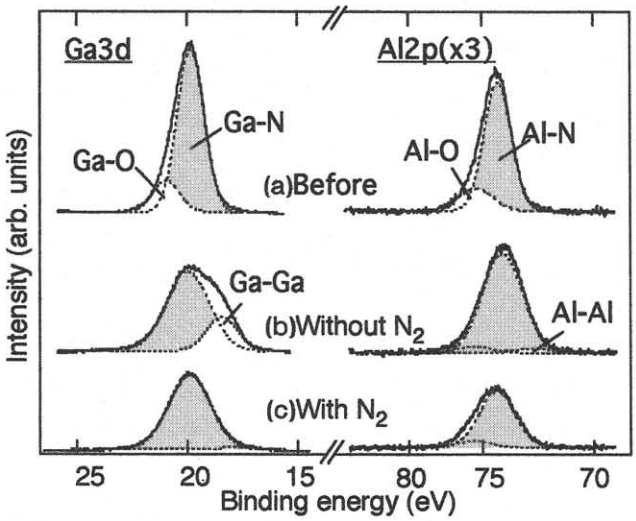

Fig. 4 XPS results of AlGaN surface (a) before etching, (b) after etching without N_2 and (c) after etching with N_2.

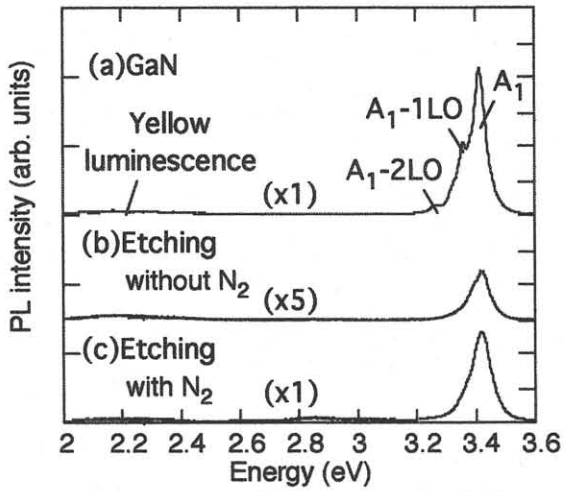

Fig. 5 PL spectra of (a) GaN sample and 3min etched AlGaN/GaN samples (b)without N_2 and (c) with N_2.

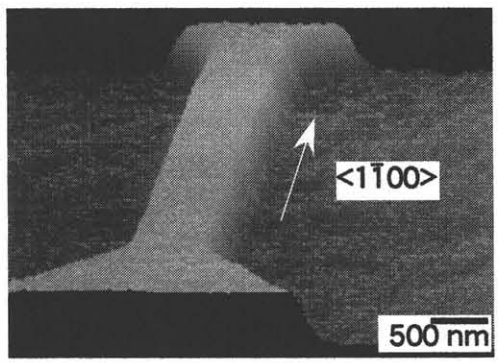

Fig. 6 AFM image of mesa-shaped AlGaN/GaN hetero structure by dry etching process.

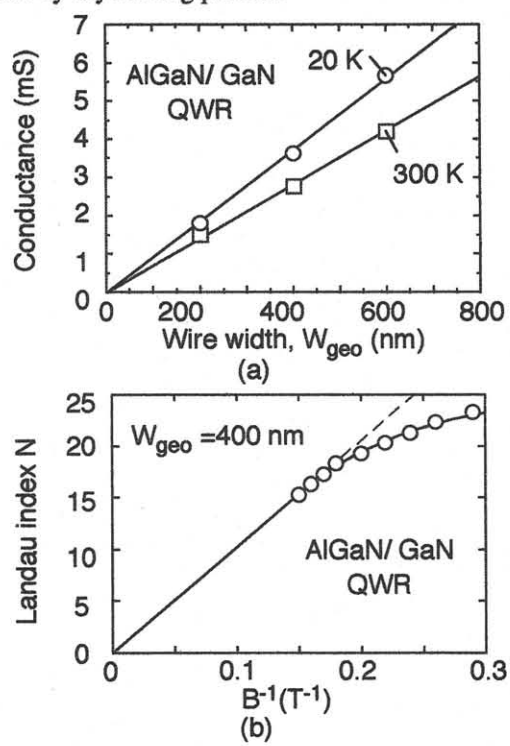

Fig. 7(a) Observed width dependence of wire conductance and (b) Landau plot of SdH oscillations.